doi:10.1111/evo.12302

PHENOTYPIC AND GENOTYPIC CONVERGENCES ARE INFLUENCED BY HISTORICAL CONTINGENCY AND ENVIRONMENT IN YEAST

Aymé Spor,[1,2,*] Daniel J. Kvitek,[3,*] Thibault Nidelet,[4,5] Juliette Martin,[6] Judith Legrand,[1] Christine Dillmann,[1] Aurélie Bourgais,[5] Dominique de Vienne,[1] Gavin Sherlock,[3] and Delphine Sicard[1,7]

[1]Univ Paris-Sud, UMR0320/UMR8120 Génétique Végétale, F-91190, Gif-sur-Yvette, France

[2]Current Address: INRA, UMR 1347, Agroecologie, F-21065 Dijon Cedex, France

[3]Department of Genetics, Stanford University, Stanford, California 94305

[4]Current Address: INRA, UMR 1083, Sciences pour l'œnologie, F-34060 Montpellier, France

[5]CNRS, UMR0320/UMR8120 Génétique Végétale, F-91190, Gif-sur-Yvette, France

[6]Université Lyon 1, Univ Lyon, France; CNRS, UMR 5086; Bases Moléculaires et Structurales des Systèmes Infectieux, IBCP 7 passage du vercors, F-69367, France

[7]E-mail: sicard@moulon.inra.fr

Received March 1, 2013
Accepted October 14, 2013

Different organisms have independently and recurrently evolved similar phenotypic traits at different points throughout history. This phenotypic convergence may be caused by genotypic convergence and in addition, constrained by historical contingency. To investigate how convergence may be driven by selection in a particular environment and constrained by history, we analyzed nine life-history traits and four metabolic traits during an experimental evolution of six yeast strains in four different environments. In each of the environments, the population converged toward a different multivariate phenotype. However, the evolution of most traits, including fitness components, was constrained by history. Phenotypic convergence was partly associated with the selection of mutations in genes involved in the same pathway. By further investigating the convergence in one gene, *BMH1*, mutated in 20% of the evolved populations, we show that both the history and the environment influenced the types of mutations (missense/nonsense), their location within the gene itself, as well as their effects on multiple traits. However, these effects could not be easily predicted from ancestors' phylogeny or past selection. Combined, our data highlight the role of pleiotropy and epistasis in shaping a rugged fitness landscape.

KEY WORDS: **Adaptive landscape, experimental evolution, life-history evolution, pleiotropy, 14-3-3 protein.**

Throughout the tree of life, evolutionarily divergent lineages have recurrently and independently evolved similar phenotypic traits. Such convergent evolution has been observed in numerous plant and animal species (Arendt and Reznick 2008; Manceau et al. 2010; Parker et al. 2013), but evidence for trait convergence is sparse in microorganisms, likely due to the paucity of visually observable phenotypes. Among the few examples of convergent evolution in microbes are the independent evolution of fruiting bodies and thallus type in microscopic fungi (Plata and Lumbsch 2011), and fermentation in yeast species (Ostrowski et al. 2008).

*These authors contributed equally to this work.

Accession Numbers

The Illumina sequence data are available at the NCBI Sequence Read Archive under accession SRA029322.1.

EVOLUTION
INTERNATIONAL JOURNAL OF ORGANIC EVOLUTION

Phenotypic convergence can be caused either by natural selection or by chance. Physical or biological constraints can restrict available phenotypes to a subset of phenotypic space (DePristo et al. 2005; Weinreich 2006; Gompel and Prud'homme 2009; Chevin et al. 2010; Feldman et al. 2012), and in this restricted space, chance alone can cause phenotypic convergence. However, if convergent evolution occurs only by chance, it will not necessarily be driven by the ecological niche of the organisms. By contrast, if natural selection drives convergent evolution, convergence may be expected in environments that share similar aspects. However, the extent to which the environment drives convergent evolution is largely unknown, as most studies have focused on either natural populations in uncontrolled environments (Arendt and Reznick 2008; Gompel and Prud'homme 2009; Elmer and Meyer 2011) or laboratory-evolved populations in a single well-controlled environment (Wichman 1999). In addition, most studies have focused on a limited number of traits, and it is unclear how convergent evolution for a single phenotypic trait is constrained by changes in correlated traits. Covariation of life-history traits (i.e., traits involved in the life cycle of an organism) and/or morphological traits has been well described (Roff 2002), with the course of evolution shaped by natural selection (Schluter 1996; Arnold et al. 2001). However, how the convergence of one trait impacts the evolution of other traits remains to be studied empirically (Kolbe et al. 2011).

On the one hand, phenotypic convergence could arise through mutations in different sets of genes that cause similar phenotypes in distinct lineages (True and Haag, 2001; David et al. 2013). Alternatively, phenotypic convergence may instead be caused by convergent or parallel evolution at the genotypic level (Wichman Arendt and Reznick 2008; Remold et al. 2008; Gompel and Prud'homme 2009; Elmer and Meyer 2011; Bedhomme et al. 2012; Feldman et al. 2012; Tenaillon et al. 2012, Wong et al. 2012; Parker et al. 2013). Parallel genotypic evolution arises when mutations occur in independent lineages that start from the same genotype, whereas convergence refers to mutations produced from different ancestral genotypes (Zhang and Kumar 1997). Parallel and convergent genotypic evolution may arise at several levels: the same nucleotide mutating independently several times (Wichman 1999; Rozpędowska et al. 2011), different mutations in the same gene (Rosenblum et al. 2010) or in a multigene family (Christin et al. 2007; Srithayakumar et al. 2011), through mutations in different genes sharing the same function (Elias and Tawfik 2012) or in the same network (Lozovsky et al. 2009). Several experimental evolutions have now analyzed genomic parallelism and convergence. This has been done primarily in virus and bacteria (Bull et al. 1997; Cunningham et al. 1997; Martinez-Picado et al. 2000; Wichman et al. 2005; Remold et al. 2008, Bedhomme et al. 2012, Tenaillon et al. 2012; Wong et al. 2012; Herron and Doebeli 2013) and less extensively in yeast (e.g., Gresham et al. 2008; Lang et al. 2013). However, how frequently complex phenotypes arise by repeated genomic and physiological pathway in different lineages is far from clear (Wood et al. 2005; Roff 2011).

Phenotypic and/or genotypic evolution can be constrained by historical factors, which can produce different phenotypic and/or genotypic outcomes despite similar environmental conditions. This has been defined as historical contingency (Travisano et al 2005, Blount et al. 2008). Historical contingency arises because the effects of mutations are contingent on the alleles that have been retained from history through epistasis. This constrains mutational paths and, as a consequence, the evolution of phenotypes. However, selection in similar environments is supposed to eliminate the effect of historical contingency on phenotype, as illustrated by the numerous examples of phenotypic convergence. As a consequence, the effects of historical contingency are expected to be detected more frequently at the genomic level, than at the phenotypic level, especially for traits correlated to fitness (Teotónio et al. 2009; Nguyen et al. 2012; Bedhomme et al. 2013; Joshi et al. 2003). Alternatively, antagonistic pleiotropy, where a mutation that is beneficial for one fitness component is deleterious for another, may decrease the effect of selection on each trait separately and may constrain the phenotypic evolution contingently to its past phenotype. An extensive study including multiple traits in multiple environments is lacking to test these hypotheses.

In this study, we have analyzed the evolution of 13 metabolic and life-history traits across multiple environments and genotypes using the budding yeast *Saccharomyces cerevisiae* as a model system. Yeast is one of the few microorganisms for which life-history traits have been studied (Spor et al. 2008, 2009; Granek et al. 2011; Magwene et al. 2011; Wang et al. 2011), and yeast populations display different life-history phenotypes depending on their ecological niche of origin (Spor et al. 2009). Using experimental evolution, we asked how selection and historical contingency interact with respect to phenotypic and genotypic evolution. We found evidence of genotypic convergence underlying multiple trait convergence in specific environments, suggesting that the mutational paths on the adaptive landscape are restricted by selection. We also found that the evolution of most traits, including different fitness components, is constrained by history. By further investigating the convergence in one gene, we demonstrate that genotypic convergence underlying multitrait convergence depends partly on the environment and partly on the ancestors' genetic background, highlighting the role of pleiotropy and history in shaping a rugged fitness landscape.

Materials and Methods

YEAST STRAINS

Six strains were chosen from the Saccharomyces Genome Resequencing Project (Table 1) that are distributed on the *S. cerevisiae* phylogenomic tree (Liti et al. 2009), and differ for several

Table 1. *Saccharomyces cerevisiae* **strains used in this study.**

Strains ID	Laboratory ID	Genetic group	Geographical origin	Habitat	Environmental source
NCYC110	247	WA	West Africa	Industrial	Ginger beer from *Z. officinale*
YJM981	304	W/E	Bergamo, Italy	Clinical isolate	Vagina
YPS128	104	NA	Pennsylvania, USA	Forest	Oak exudate
UWOPS83-787.3	270	Mosaic	Bahamas	Fruit	*Opuntia stricta*
S288C	96	Mosaic	California, USA	Laboratory	Rotting fig
Y55	97	Mosaic/WA WA	France	Laboratory	Wine

Genetic groups were obtained from inference of *S. cerevisiae* population structure using the program Structure (Liti et al. 2009). WA, West Africa; W/E, Wine/European; NA, North America; Mosaic/WA, Mosaic, mostly West African.

life-history and metabolic traits (Spor et al. 2008, 2009). They are all homothallic autodiploids, except S288c, which is haploid. For each phenotypic evaluation, a single new colony was isolated from the −80°C stock.

EXPERIMENTAL EVOLUTION

Three replicates of each of the six strains were serially propagated (2 ml into 40 ml of fresh liquid medium) under four selection regimes over 5 months. Two different glucose conditions (1% and 15% glucose in 3% YNB with amino acids) and two different "winter" lengths (48 h and 96 h) were chosen. The cultures were incubated at 30°C at 200 rpm. In 1% glucose, the yeast populations first grow fermentatively and then switch to respirative growth after the diauxic shift. Cycles of 48 h have a very short period of respiration, unlike the cycles of 96 h. In 15% glucose, the yeast populations grow only fermentatively but are subject to osmotic stress. Cycles of 48 h are composed of a long period of growth followed by a short period of stationary phase whereas cycles of 96 h have a long stationary phase. The four selection regimes are denoted 1%_48h, 1%_96h, 15%_48h, and 15%_96h. All six strains were propagated in these four conditions in triplicate. Over 5 months, the populations transferred every 48 h were transferred 74 times (about 325 generations), whereas the populations transferred every 96 h were transferred 37 times. At each transfer, the populations were diluted 20-fold leading to an effective population size ranging from 106 to 107 depending on the strain and the selection regime. Of the 72 evolved populations, 12 were discarded due to cross-contamination, as detected using microsatellite analysis. The 60 remaining evolved population included a duplicate of evolution for all ancestors strains in all four selection regimes, except for strain S288c (the haploid strain) in the 1_48h and 15_48h selection regimes and for strain YJM981 in the 1_96h selection regime.

PHENOTYPING ANCESTRAL STRAINS AND EVOLVED POPULATIONS

Phenotyping of two clones from each of the six ancestral strains and a single-end clone from each of the 60 evolved populations was performed in both 1% and 15% glucose as described in Spor et al. (2009), leading to a total of 144 sets of phenotyping kinetics. For each kinetic, nine life-history (reproduction rate in fermentation R_{ferm}, time to diauxic shift T_{shift}, reproduction rate in respiration R_{resp}, carrying capacity K_{ferm} and cell size S_{ferm} at the diauxic shift time point, population sizes *PopSize48h*, *PopSize96h*, and cell sizes *S48h*, *S96h* measured at the serial transfer time points) and four metabolic traits (specific glucose consumption rate denoted J_{spec} ($g \times min^{-1} \times cell^{-1}$), ethanol amount denoted *Eth48h* and *Eth96h* expressed in $g \times l^{-1}$ and yield Y_{ferm}, measured as the ratio of the biomass to the quantity of glucose consumed) were quantified.

STATISTICAL ANALYSIS

Response to selection

Phenotyping was realized during 144 population dynamics (60 evolved populations + 6 × 2 repetitions of ancestors × 2 media conditions), randomly distributed into five blocks of experiments. For each trait Z, the phenotypic evolution was calculated as follows:

$$\Delta Z_{ijklm} = \frac{Z_{evolved_{ijklm}} - \overline{Z}_{ancestral_{il}}}{\overline{Z}_{ancestral_{il}}},$$

where the value of the ancestral strain is averaged over the replicates.

Variation of each variable ΔZ among media and strains was first analyzed using the following mixed model of analysis of variance (ANOVA):

$$\begin{aligned}\Delta Z_{ijklm} = {} & \mu + Block_m + eval\,medium_l \\ & + ancestors_i + selection\,regime_j \\ & + (eval\,medium \times ancestors)_{il} \\ & + (eval\,medium \times selection\,regime)_{jl} \\ & + (ancestors \times selection\,regime)_{ij} + \varepsilon_{ijklm},\end{aligned}$$

where ΔZ is the variable, *Block* is the random block effect (experimental repetition, $m = 1, 2, 3, 4, 5$), *eval medium* is the

evaluation condition effect (l = 1, 2), *strain* is the diploid strain effect ($i = 1, 2, 3, 4, 5$), *selection regime* is the selection regime effect ($j = 1, 2, 3, 4$), *eval medium* × *strain* (fixed), *eval medium* × *selection regime* (fixed) and *strain* × *selection regime* (fixed) are interaction effects, and ε is the residual error. The interaction effects were chosen to study the interactions between the historical contingency (ancestors' effect) and selection effects. To account for multiple testing, the significance of the different effects was assessed using the false discovery rate (FDR) method (Benjamini and Hochberg 1995).

For each trait, normality and homogeneity of residual distributions were checked. Least square means and REML variance estimates were obtained using the JMP® software. The significance of differences between selection regime means was assessed using the Tukey HSD method.

Identifying convergence and divergence

To study further the phenotypic landscape of our evolved strains, we performed linear discriminant analyses (LDAs) of the 13 traits for each evaluation medium. However, prior to those analyses, we corrected the data for a block effect estimated by a simple regression model performed trait by trait and for each evaluation medium separately. Missing values were replaced by the mean over replicates of evolution. The *PopSize48h*, *PopSize96h*, and K_{ferm} were $\log_{10}$ transformed. We analyzed separately the data obtained with the two evaluation media. We discarded the S288c strain from those analyses, as it was the single haploid strain. In some cases, respiration did not occur and/or the reproduction rate in respiration (R_{resp}) could not be easily estimated. In these cases, the R_{resp} was considered to be zero. However, we did not include the null values to estimate the block effect. For one block, the block effect could not be estimated, as all R_{resp} values were null. For this block, the R_{resp} values were replaced by the averaged R_{resp} (corrected for block effects) over strains evolved in the same selection regime from the same ancestor strain. An alternative would have been to replace those R_{resp} values by the average over all null R_{resp} corrected for block effects. We checked that using this alternative did not affect the results.

The four selection regimes defined the four categories used a priori to compute the discriminant functions. The a posteriori assignment probabilities to a priori categories indicate if the objects can be properly assigned to an a priori group. After using the data of diploid evolved strains to build the axes of the LDA, the ancestral strains as well as the evolved strains (including the haploid discarded S288c strain) were projected on those axes. The output of the analyses in each evaluation medium ($l = 1, 2$) were the coordinates of each strain evolved in each selection regime ($j = 1, 2, 3, 4$) as well as the coordinates of each ancestor strain. The axes of the LDA represent a linear combination of the traits that discriminate the most selection regimes. Hence, the traits that correlate with the axes are those for which convergence was observed within a selection regime and divergence was observed between selection regimes. To account for multiple testing, the significance of correlations was assessed using the FDR method. To identify whether the selection regime and the genetic background of the ancestor had an impact on the traits, we carried out a MANOVA on the 13 traits and test for an ancestral effect, a selection regime effect and an ancestral by selection regime interaction effect. Those analyses were conducted on the same data as the LDA.

DETERMINING THE GENOTYPE OF EVOLVED CLONES

Whole-genome sequencing and SNP/indel detection

Genomic DNA was extracted from final clones either by spooling (Treco 1987), or using Qiagen G/100 Genomic Tips. Single-end Illumina sequencing libraries were generated using the Illumina Genomic DNA Sample Prep Kit starting with 5 μg of genomic DNA, and sequencing flow cells were prepared using the Illumina Standard Cluster generation Kit. Samples were sequenced on the Illumina Genome Analyzer II, generating 36 bp reads. The data were mapped to the S288c reference (from SGD, Dec 3, 2008) and to additional contigs generated from other *S. cerevisiae* strains (Dunn et al. 2012) using BWA version 0.5.8 (Li and Durbin 2009) with default parameters.

SNP calling was performed on uniquely mapping reads only using the Genome Analysis Toolkit version 1.0.4905 (McKenna et al. 2010) on all strains simultaneously with ad hoc quality filtering (see Supporting Information Material and methods). SNPs were validated using Sanger sequencing.

Indels were called using Samtools version 0.1.7 (Li et al. 2009) with default settings; the false positive rate was decreased using an in-house developed method (see Supporting Information Material and methods). Indels were validated using Sanger sequencing.

Copy number variation (CNV) detection

Sequence coverage was used to identify CNVs between each evolved and ancestral strain pair as in Araya et al. (2010). Briefly, raw sequencing coverage was averaged over 25 bp segments across the genomes of each evolved clone and ancestor and $\log_2$(evolved/ancestor) ratios were calculated. These $\log_2$ ratios were then adjusted by either the genome-wide $\log_2$ mean to identify whole-chromosome CNVs, or each chromosome's $\log_2$ mean to identify intrachromosomal CNVs. Genome segments were identified using the R package DNAcopy version 1.22.1 (Venkatraman and Olshen 2007) with default parameters except: smooth.CNA(smooth.region = 5); segment(min.width = 5, undo.splits = "sdundo," undo.SD = 4). Results of DNAcopy were plotted and regions of varying copy number were identified visually. Putative CNVs occupying partial chromosomes were

tested using real-time quantitative PCR of genomic DNA as described (Hoebeeck et al. 2007), except that each putative CNV was normalized to a single nonvarying locus located on the same chromosome as the putative CNV. The whole-chromosome 15 CNV in Y55:15%_48h was normalized to a single nonvarying locus on a different chromosome.

Gene Ontology (GO) enrichment analysis

GO biological process enrichments were determined using GO: TermFinder (Boyle et al. 2004) at SGD (http://www.yeastgenome.org) using default parameters, except dubious open reading frames (ORFs) were omitted from the analysis, with a FDR cutoff of 0.05. All genes containing at least one mutation within its ORF were included.

CONVERGENCE ON *BMH1*

Testing the presence of selection on BMH1

We built a theoretical model of our experimental evolution and computed the probability of observing recurrent *BMH1* mutations among M-evolved clones at the end of our experimental evolution under the hypotheses that there is no selection. We considered the experimental evolution as J cycles of k generations. We assume that the rate of mutation per nucleotide at each generation is $\mu 0 =$ 10-10. For one given cycle with an initial frequency p of *BMH1* mutation (gene of length $l = 803$ bp), we estimated that the frequency of mutants after k generations is $q = 1 - (1 - p)(1 - (1 - (1 - \mu 0)2l)/2)k$. Each cycle is separated by a bottleneck. To simulate the impact of bottlenecks at each cycle, we considered that the number of mutants at the beginning of the ith cycle follows a Poisson distribution with mean $qi - 1Ni$, where Ni is the number of cells at the beginning of the cycle and $qi - 1$ is the frequency of mutants at end of the $(i - 1)$th cycle. To keep a stable population at the beginning of each cycle ($Ni = N0 = 10^6$), we assumed that the number of generations per cycle is $k = \log(D)/\log(2)$ with D the factor of dilution ($D = 20$). With this model, we simulated 107 experimental evolutions mimicking the experimental evolution of each of our two types of selection regimes (transfer every 96 h leading to 35 cycles of evolution and transfer every 48 h leading to 70 cycles of evolution). By simulating 107 experimental evolutions of M1 = 32 populations (respectively, M2 = 28 populations) with J1 = 35 cycles (respectively, J2 = 70 cycles), we estimate the probability of observing m mutants in the same gene of length 802 bp under the null hypotheses that there is no selection.

BMH1: Structure and docking predictions

We generated a structural model of yeast dimeric Bmh1p to locate the amino acid changes and truncation on the 3D protein structure. We used its homology with the human protein 2BR9, whose structure has been resolved by crystallography (Yang et al. 2006, see Supporting Information and Material and methods). Arbitrary and specific docking predictions were then carried out (see Supporting Information and Material and methods).

Evaluating the impact of BMH1 mutations

We tested for the effect of *BMH1* mutations on Z the value of a single trait in an evolved population. We used the following linear model:

$$\begin{aligned} Y_{ijlb} = \mu &+ eval\,medium_l + Bmh1p_b \\ &+ selection\,regime_j \\ &+ (Bmh1p \times eval\,medium)_{lb} \\ &+ (Bmh1p \times selection\,regime)_{jb} \\ &+ (eval\,medium \times selection\,regime)_{jl} \\ &+ (Bmh1p \times eval\,medium \\ &\times selection\,regime)_{ljb} + \varepsilon_{ijlb}, \end{aligned} \quad (1)$$

where Y_{ijlb} is Z, *eval medium* is the effect of the culture medium ($l = 1, 2$), *selection regime* ($j = 1, 2, 3, 4$) is the effect of the selection regime, *Bmh1p* is the effect of mutations in Bmh1p ($b = 1, 2, 3, 4, 5$), $(Bmh1p \times eval\,medium)_{lb}$, $(Bmh1p \times selection\,regime)_{jb}$, $(eval\,medium \times selection\,regime)_{jl}$, $(Bmh1p \times eval\,medium \times selection\,regime)_{ljb}$ interaction effects, and ε_{ijlb} is the residual error. The effects of the Bmh1p protein changes (*Bmh1p* effect) were tested from the ANOVA using contrast. FDR corrections were carried out using a value of 15%. For three traits (Y_{ferm}, *Eth*_48h, *Eth*_96h), the ANOVA was carried out separately for each evaluation medium because of residuals heteroscedasticity.

This ANOVA model using *BMH1* as sole genetic information was compared to the following model using the genetic differences between ancestral strains:

$$\begin{aligned} Y_{ijl} = \mu &+ eval\,medium_l + Strains_i + selection\,regime_j \\ &+ (Strains \times eval\,medium)\,li \\ &+ (Strains \times selection\,regime)_{ji} \\ &+ (evalmedium \times selection\,regime)_{jl} \\ &+ (Strains \times eval\,medium \\ &\times selection\,regime]_{ijl} + \varepsilon_{ijl}. \end{aligned}$$

Similar R^2 between the two models would indicate that genetic variation in the gene where genetic convergence occurred explained as much traits variation than genome differences between evolved strains.

Table 2. Analysis of variance of the relative response to selection of each life-history and metabolic trait.

		K_{ferm}		*PopSize48h*		*PopSize96h*		S_{ferm}		*S48h*		*S96h*	
Source	df	*F*	*P*	*F*	*P*	*F*	*P*	*F*	*P*	*F*	*P*	*F*	*P*
Block	5	5	**5×10^{-4}**	4.7	**8×10^{-4}**	9.4	**6×10^{-07}**	1.1	0.35	2.8	**0.024**	1	0.42
eval medium	1	259.6	**7×10^{-26}**	19.9	**3×10^{-5}**	0.003	0.95	128.7	**6×10^{-18}**	116.4	**6×10^{-17}**	1.3	0.26
Strain	4	6.6	**1×10^{-4}**	19.2	**7×10^{-11}**	7.1	**7×10^{-5}**	9.1	**5×10^{-6}**	32.6	**1×10^{-15}**	13.7	**2×10^{-8}**
Selection regime	3	3.6	**0.017**	8.1	**9×10^{-5}**	10.6	**7×10^{-6}**	8.9	**4×10^{-5}**	40.2	**1×10^{-15}**	20.9	**6×10^{-10}**
eval medium × strain	4	13.1	**4×10^{-8}**	5.5	**6×10^{-4}**	24.1	**8×10^{-13}**	37.2	**4×10^{-17}**	27.8	**4×10^{-14}**	13.2	**3×10^{-8}**
eval medium × selection regime	3	0.84	0.48	1.5	0.216	7.7	**1×10^{-4}**	4	**0.01**	14.4	**2×10^{-7}**	2.2	0.1
strain × selection regime	12	0.94	0.52	1.9	0.05	3.5	**4×10^{-4}**	4	**10^{-4}**	2.95	**0.002**	2.3	**0.017**
Residuals means square		0.1		0.027		0.046		0.002		0.001		0.002	

		R_{ferm}		R_{resp}		T_{shift}		J_{spec}		Y_{ferm}		*Eth48h*		*Eth96h*	
Source	df	*F*	*P*	*F*	*P*	*F*	*P*	*F*	*P*	*F*	*P*	*F*	*P*	*F*	*P*
Block	5	15.2	**3×10^{-10}**	3.01	**0.016**	13.67	**2×10^{-9}**	0.77	0.552	3.8	**0.004**	4.92	**6×10^{-4}**	1.24	0.300
eval medium	1	18.4	**5×10^{-5}**	0.75	0.39	56.28	**1×10^{-10}**	2.23	0.141	236	**2×10^{-24}**	177.65	**2×10^{-21}**	37.27	**4×10^{-8}**
Ancestor	4	9.6	**2×10^{-6}**	4.11	**0.005**	1.96	0.11	13.4	**8×10^{-8}**	7.5	**4×10^{-5}**	60.83	**8×10^{-23}**	12.53	**7×10^{-8}**
Selection regime	3	3.4	**0.02**	0.51	0.68	5.51	**0.002**	3.8	**0.014**	3.2	**0.027**	4.87	**0.004**	12.98	**6×10^{-7}**
eval medium × strain	4	6.8	**1×10^{-4}**	1.87	0.13	1.79	0.14	13.3	**9×10^{-8}**	10	**2×10^{-6}**	58.33	**3×10^{-22}**	3.45	**0.012**
eval medium × selection regime	3	1.28	0.28	2.29	0.085	1.7	0.18	3.25	**0.028**	0.35	0.79	4.40	**0.007**	12.14	**1×10^{-6}**
ancestor × selection regime	12	1.80°	0.063	0.48	0.92	1.81	0.063	1.88°	0.056	0.55	0.88	2.31	**0.014**	1.62	0.104
Residuals		0.02		0.05		0.01		3.59		0.09		1.92		0.05	

Source **is the tested effect, df is the degree of freedom. *MS* is the mean square and *F* is the Fisher's *F*. The significant *P* values after FDR correction (global level 0.05) are indicated in bold.**

Results

We chose six diverse *S. cerevisiae* strains for which there exists whole-genome sequence, with the goal of maximizing habitat of origin and genetic and phenotypic variability (Spor et al. 2008, 2009; Liti et al. 2009; Table 1). Three replicates of each strain were propagated in serial batch cultures under four selection regimes (1%_48h, 1%_96h, 15%_48h, and 15%_96h) differing by the glucose content (1% or 15%) and by the cycle length (48 h or 96 h). The 48 h and 96 h cycle length experiments were stopped after at least 325 or 165 generations, respectively. At the end of the experiment, we studied nine life-history traits (growth rates during fermentation [R_{ferm}] and respiration [R_{resp}], the time to diauxic shift [T_{shift}], population sizes at T_{shift} and the serial transfer time points [K_{ferm}, *PopSize48h*, *PopSize96h*], and cell sizes at T_{shift} and serial transfer time points [S_{ferm}, *S48h*, and *S96h*]), and four metabolic traits (the specific glucose consumption rate [J_{spec}], the biomass yield from fermentation [Y_{ferm}], and the quantity of ethanol produced and released in the medium at the two serial transfer time points [*Eth48h* and *Eth96h*]).

PHENOTYPIC RESPONSES TO SELECTION

We analyzed each strain for the evolution of each trait relative to its ancestral population using mixed-effects ANOVA (see Material and Methods). The selection regime effect, which measures the differences in phenotypic evolution between the four selection regimes, across all strains, was significant for all traits except R_{resp}, indicating that the strains evolved toward different phenotypes depending on the selection regime (Table 2). We summarize the response to selection in each selection regime using the average trait evolution across all strains (Table 3). A value of 0 indicates no detectable response to the selection on average, whereas a positive (negative) value indicates an increase (decrease) of the average value of the trait in the evolved populations compared to the ancestral strains. The strongest response to selection occurred in the selection regime with the strongest glucose starvation, that is, the 1%_96h selection regime. The 1%_96h regime selected for decreased cell size S and increased population size (*PopSize*), which tends to previously described life-history traits values found among strains originating from soil and oak bark (Spor et al. 2009). Populations selected under this regime also displayed an increase of R_{ferm} and J_{spec}. The 1%_48h regime selected for an intermediate life-history phenotype that is close to the average life-history phenotype of the ancestral populations at 48 h (*PopSize48h* and *S48h* are near zero), however the characteristics of the evolved population are different regarding the traits in fermentation (increased R_{ferm}, K_{ferm}, J_{spec}, and decreased S_{ferm}, Tables 2 and 3). Globally, both 1% regimes selected for a decreased cell size compared to the 15% regimes. The difference in cycle lengths (48 h vs. 96 h) mainly led to the evolution of metabolic

Table 3. Main effect of the selection regime on the relative response to selection of life-history and metabolic traits.

Selection regime	K_{ferm}	*PopSize48h*	*PopSize96h*	S_{ferm}	*S48h*	*S96h*	R_{ferm}	R_{resp}	T_{shift}	J_{spec}	*Eth48h*	*Eth96h*	Y_{ferm}
1%_48h	1.1^{A}	0.088^{B}	0.569^{B}	-0.137^{BC}	-0.070^{B}	-0.061^{B}	0.083^{A}	NS	-0.030^{B}	1.467^{A}	0.73^{A}	-0.381^{C}	0.67^{A}
1%_96h	1.08^{AB}	0.247^{A}	0.832^{A}	-0.160^{C}	-0.115^{C}	-0.098^{C}	0.060^{AB}	0.113^{A}	0.013^{B}	0.4^{AB}	1.72^{A}	-0.208^{B}	0.713^{A}
15%_48h	0.87^{AB}	-0.018^{B}	0.499^{B}	-0.085^{A}	-0.003^{A}	-0.018^{A}	0.021^{AB}	0.085^{A}	-0.028^{B}	1.61^{AB}	1.61^{A}	-0.239^{C}	0.514^{A}
15%_96h	0.82^{B}	0.013^{B}	0.461^{B}	-0.116^{AB}	-0.012^{A}	-0.008^{A}	-0.03^{B}	0.069^{A}	0.070^{A}	0.155^{B}	1.61^{A}	-0.004^{A}	0.554^{A}

Mean relative response to selection is given for each trait in each selection regime. For each trait, significance of the differences was assessed by HSD Tukey tests. Levels that are not connected by a common letter (A, B, or C) are significantly different.

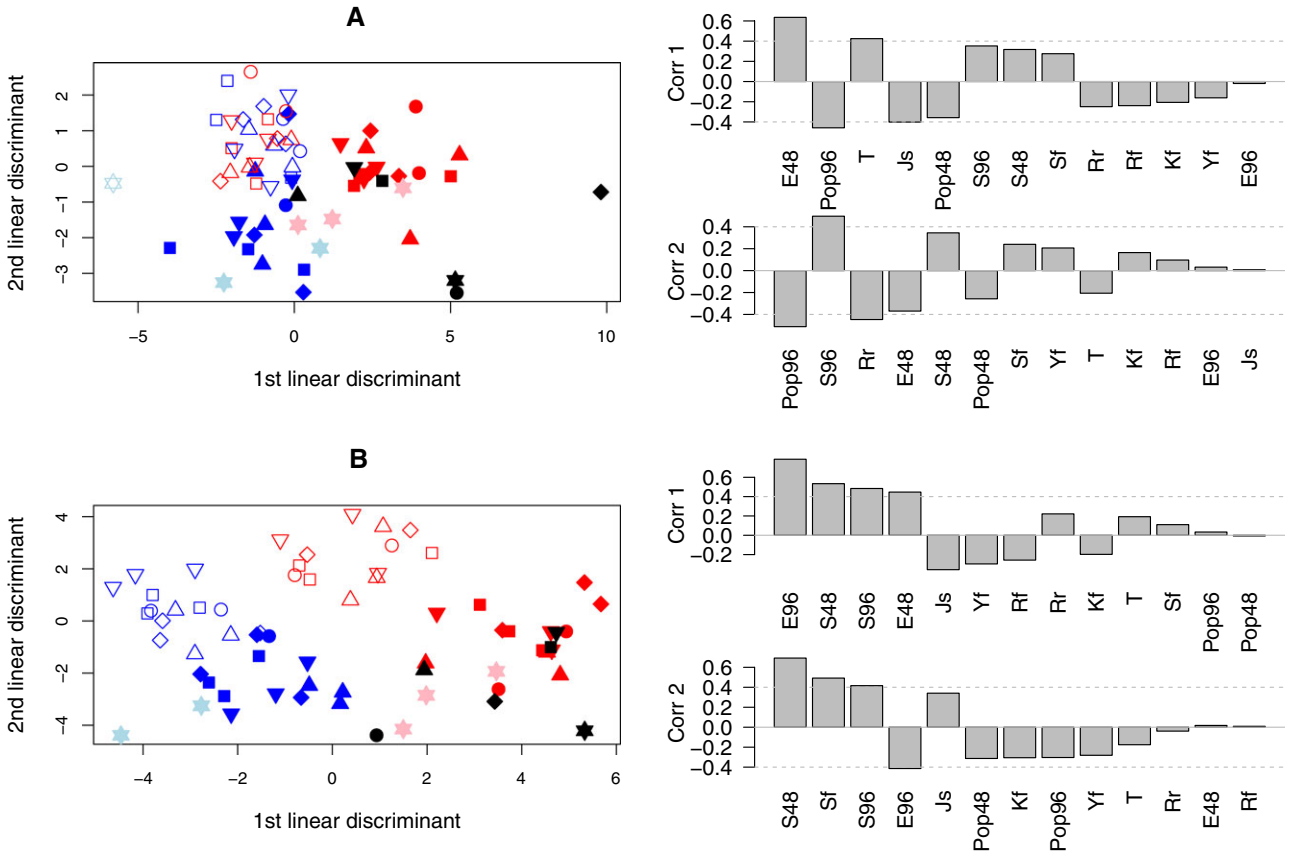

Figure 1. Canonical plots of the linear discriminant analysis. (A) Phenotypic evaluation of ancestral strains and evolved populations in the 1% glucose medium. (B) Phenotypic evaluation of ancestral strains and evolved populations in the 15% glucose medium. The correlations between traits and how they explain the linear discriminant axis are presented on the right. The colors of the symbols correspond to the different selection regimes (empty blue, 1%_48h; filled blue, 1%_96h; empty red, 15%_48h; and filled red, 15%_96h). The black symbols correspond to the ancestral strains. The shapes of the symbols correspond to the evolved and ancestral state of a given strain (stars for S288c, down triangle for Y55, up triangle for YPS128, diamond for NCYC110, square for UWOPS83-787.3, and circle for YJM981). The traits were denoted as follows: reproduction rate in fermentation R_f, time to diauxic shift T, reproduction rate in respiration R_r, carrying capacity K_f, cell size at the diauxic shift time point S_f, population sizes *Pop48*, *Pop96*, cell sizes *S48*, *S96*, and ethanol amounts *E48* and *E96* measured at the serial transfer time points, specific glucose consumption rate J_s, and yield Y_f.

changes—both 96h cycle length regimes selected for populations that left more residual ethanol compared to the 48h cycle length regimes. In 15% glucose regimes, the 96h regime also selected for an increase in the amount of time spent in fermentation (T_{shift}) with a decrease in the glucose consumption rate (J_{spec}).

MULTIPLE TRAITS CONVERGENCE WITHIN SELECTION REGIMES

To determine which traits converged most within a selection regime and diverged most between selection regimes, we carried out one LDA on all traits for each evaluation medium (1% and 15% glucose, respectively, Fig. 1A and 1B) setting the four selection regimes as four a priori categories. The LDA axes represent the combination of life-history trait values toward which directional selection has driven the populations in each selection regime, that is, the multivariate phenotypic convergence landscape. The first two axes explained 89.1% and 95.9% of the variance in 1% glucose and 15% glucose evaluation media, respectively. The probability of a population being correctly assigned to its selection regime was 0.99 in the 15% glucose evaluation medium, indicating convergence within selection regime and diversifying selection among selection regimes for several traits (see Fig. 1B). This probability was 0.88 in the 1% glucose evaluation medium as we were not able to discriminate between the 1%_48h regime and the 15%_48h regime (see Fig. 1A). Among the 13 traits, cell size (*S96h*, *S48h*, S_{ferm}), traits related to fitness during the respiration phase (*PopSize96h*, *PopSize48h*, R_{resp}), as well as metabolic traits (J_{spec}, *Eth48h*, *Eth96h*, T_{shift}) were significantly correlated to at least one of the LDA axes indicating that they were the most convergent traits within selection regime and divergent traits between selection regimes. By contrast, the traits related to fitness during fermentation (R_{ferm}, K_{ferm}, Y_{ferm}) did not significantly

explain any of the axes of the phenotypic convergence landscape. Indeed, these traits evolved toward the same points in the different selection regimes.

EFFECT OF HISTORICAL CONTINGENCY ON PHENOTYPIC CONVERGENCE

The effect of historical contingency was tested by a MANOVA performed on all traits of the evolved populations evaluated either in the 1% glucose or in the 15% glucose media. The ancestor effects were significant in both evaluation media (Pillai = 1.5, $P < 0.001$ in 1% glucose media; Pillai = 1.9, $P < 0.001$ in 15% glucose media). An ancestor effect was found separately for each trait except for T_{shift} and *Eth48h* in the 1% glucose evaluation medium and for R_{ferm}, R_{resp}, *Eth48h* in the 15% glucose evaluation medium (Table S1). In 14 cases of the 26 evaluated traits (13 traits in two evaluation media), an interaction effect between selection regime and ancestor effect was found, indicating that the ancestor effect may depend on the environment (Table S1).

We then asked whether ancestral strains that were phenotypically more similar evolved more similar phenotypes. We measured the distances between pairwise ancestral strains and the distances between the derived pairwise evolved populations in each selection regime and tested their correlation using Mantel tests and FDR methods to account for multiple testing. The distances were computed using two different metrics: the LDA axes or each trait. On the LDA axis, we did not find any significant correlation between the phenotypic distances of evolved populations and their ancestors' ones. When analyzing each trait separately, only five of the 52 correlation tests (13 traits × 4 selection regimes) were significant indicating that phenotypic evolution cannot be predicted easily from the ancestors' phenotype. Significant correlations were found for S_{ferm} in the 15%_96h selection regime ($r = 0.7, P < 0.001$) as well as K_{ferm} ($r = 0.76, P < 0.001$), *PopSize96h* ($r = 0.62$, $P = 0.002$), Y_{ferm} ($r = 0.59$, $P = 0.003$), and *Eth96h* ($r = 0.69, P < 0.001$) in the 1%_96h selection regime. We did not find any significant correlations between the phenotypic distances of evolved populations and the phylogenetic relationships of their ancestral strains.

GENOTYPIC RESPONSE TO SELECTION

To determine if genotypic convergence was underlying the observed phenotypic convergence, we sequenced the genomes of the ancestral strains Y55, YPS128, UWOPS83-787.3, and YJM981, and of clones that were evolved in the 1%_48h and 15%_48h conditions, for a total of eight ancestral-evolved pairs. We identified 27 SNPs and indels across the eight evolved clones relative to their respective ancestor (Table 4).

The vast majority of SNPs were nonsynonymous changes (21/27). Of the remaining mutations, three were synonymous changes in protein sequences, and three were located in intergenic regions. Of the 21 nonsynonymous variants, 10 were nonsense mutations and 11 were missense mutations. Unlike nonsense mutations, which typically result in loss of protein or domain function, missense mutations may cause loss of function, gain of function, or no functional change. Of the 11 missense mutations, SIFT (Kumar et al. 2009) predicted that six would disrupt protein function, four would be tolerated, while one had insufficient homology data for an accurate prediction. Assuming that protein-modifying mutations are most likely to influence phenotype, these data suggest that 59% of all found variants (16/27) most likely cause the evolved phenotypes, with at least one protein-modifying mutation per evolved clone.

We found evidence of seven CNVs in the evolved clones relative to their ancestral strain (Fig. 2), with four in YPS128 evolved in 1%_48h strain alone. Three of these four increase copy number, most likely resulting from a heterozygous duplication event, while the other CNV is likely a heterozygous deletion. All four CNVs are in telomeric or subtelomeric regions. The three remaining CNVs each occur in one strain apiece. Lastly, chromosome 15 appears to be a homozygously duplicated, creating two extra copies, in Y55 evolved in 15%_48h.

CONVERGENCE ON GENES INVOLVED IN SAME FUNCTION OR PATHWAY

We determined whether there were GO enrichments (Boyle et al. 2004) for the genes mutated across all strains (Table 5). GO enrichments shared by both the 1%_48h and 15%_48h conditions include "general signal transduction" as well as "Ras protein signal transduction," indicating genetic convergence in genes involved in these pathways.

The 1%_48h condition was enriched for the GO terms "signal transduction," "MAPKKK cascade," and "cellular response to stimulus" (Table 5). The drivers of these enrichments were *BMH1, PKH1, SSK2*, and *SOG2*. Of these, only *BMH1* obviously functions in nutrient signaling (Burbelo and Hall 1995; Bertram et al. 1998). The others are involved in cell wall integrity and osmolarity sensing through the HOG pathway.

The 15%_48h condition did not have significant GO enrichments when all mutated genes were considered, but when only genes with protein-modifying mutations were used, "mitotic cell cycle" was enriched (Table 5). This enrichment was driven by *TPD3, BMH1, TVP38*, and *CDC25*. Tpd3p is a regulatory subunit of protein phosphatase 2A (PP2A) and is required for transcription by RNA pol III (van Zyl et al. 1992), which when mutated results in larger cell size (Jorgensen 2002), as well as a general decrease in resistance to stress (Auesukaree et al. 2009). We observed a nonsense mutation in the clone evolved from Y55 in the 15%_48h condition, which may cause the larger cell size characteristic of the 15%_48h phenotype. Cdc25 activates Ras by phosphorylation of GDP, leading to increased signaling through the cAMP/PKA

Table 4. Characteristics of the mutations discovered in the evolved populations.

Strain : selection regime	Chromosome	Position	Parent genotype	Evolved genotype	Systematic name	Gene name	Mutation effect	Functional effect
Y55: 1%_48h	5	546253	C/C	C/G	YER177W	*BMH1*	Y 216*	Nonsense
	13	470745	G/G	G/C	YMR102C		S 536*	Nonsense
Y55: 15%_48h	1	126548	C/C	C/T	YAL016W	*TPD3*	Q 557*	Nonsense
	2	9561	C/C	C/T	5′ of tL(UAA)B1; 3′ of YBLWdelta3			Intergenic
	4	1015447	T/T	T/A	YDR277C	*MTH1*	I 85 F	Disruptive
	6	201121	G/G	G/T	YFR023W	*PES4*	Silent	Synonymous
	12	21757	G/G	G/A	YLL060C	*GTT2*	P 28 L	Disruptive
	14	451643	G/G	G/T	YNL092W		M 257 I	Tolerated
	16	488074	G/G	G/A	YPL033C	*SRL4*	Silent	Synonymous
YPS128: 1%_48h	14	220425	G/G	G/A	5′ of *URE2*; 3′ of JJJ1			Intergenic
	15	998511	G/G	A/A	YOR353C	*SOG2*	T 772 I	Disruptive
YPS128: 15%_48h	4	1333026	C/C	T/T	YDR435C	*PPM1*	E 313 K	Disruptive
	11	604204	C/C	C/G	YKR088C	*TVP38*	R 286 T	Tolerated
	12	229054	G/G	G/T	YLR040C		A 177 D	Tolerated
	15	496908	T/T	A/A	YOR092W	*ECM3*	L 594*	Nonsense
	15	497041	C/C	A/A	5′ of *ECM3*; 3′ of YOR093C			Intergenic
UWOPS83-787.3: 1%_48h	5	546126	G/G	T/T	YER177W	*BMH1*	G 174 V	Disruptive
	7	965094	*/*	+T/+T	YGR237C		Protein truncation	Nonsense
	14	682330	*/*	+T/+T	YNR031C	*SSK2*	Protein truncation	Nonsense
UWOPS83-787.3: 15%_48h	5	546138	A/A	G/G	YER177W	*BMH1*	N 178 S	Disruptive
	15	824405	*/*	−G/−G	YOR267C	*HRK1*	Protein truncation	Nonsense
YJM981: 1%_48h	4	1433639	*/*	*/+G	YDR490C	*PKH1*	Protein truncation	Nonsense
	5	546294	T/T	T/G	YER177W	*BMH1*	L 230*	Nonsense
	10	430543	T/T	T/A	YJL005W	*CYR1*	Silent	Synonymous
	12	849668	C/C	C/A	YLR361C-A		S 4 I	NA
	13	409669	G/G	G/T	YMR070W	*MOT3*	A 173 S	Tolerated
YJM981: 15%_48h	12	753687	C/C	C/T	YLR310C	*CDC25*	W 1103*	Nonsense

pathway, which stimulates progression through the cell cycle (Broek et al. 1987). The *CDC25* mutation in the evolved clone of YJM981 under the 15%_48h condition is a nonsense mutation, likely resulting in reduced Ras activity and decreased signaling through the cAMP/PKA pathway.

GENOTYPIC CONVERGENCE AT THE *BMH1* LOCUS

Because four out of the eight sequenced clones had *BMH1* mutations (Table 4), we determined whether there were *BMH1* mutations in the other evolved populations, and also sequenced BMH2, which encodes a paralogous protein of the 14-3-3 protein family. No mutations were detected in *BMH2*, but 12 of the 60 clones had *BMH1* mutations (Fig. 3A), with eight being heterozygous for the mutant allele and four being homozygous. The 12 mutations were distributed across nine sites and can be grouped in two classes: six mutations are STOP mutations that occurred between positions 642 and 690 bp downstream from the ATG, and six mutations are nonsynonymous mutations that mostly occurred at 522–534 bp from the ATG (Fig. 3A). At one site, the exact same mutation occurred twice independently.

Using a mathematical model, we checked whether the number of *BMH1* mutations observed at the end of the experimental evolution could be found under the hypotheses that there is no selection. By simulating 107 experimental evolutions of M1 = 32 populations (respectively, M2 = 28 populations) with 34 bottlenecks (96h selection regime) or 69 bottlenecks (48h selection regime), we estimated, under the null hypotheses that there is no selection, that the probabilities of observing four mutants after evolution in the 96h selection regime or eight mutants after evolution in the 48h selection regime were below 10-7, indeed suggesting that selection is responsible.

BMH1 mutations were found in Y55, YJM981, UWOPS83-787.3 but not in the other ancestor strains, leading to a significant ancestor effect on convergence (Fig. 3A and 3B, Fisher's exact test, $P = 0.005$). Among the two types of *BMH1* mutations, STOP mutations were preferentially retained in W1 ancestral allele whereas missense mutations were preferentially retained in W2 allele (Table 6, Fig. 3). However, the occurrence of *BMH1* mutations does not appear to be related to the genomic distance between the ancestral strains (Fig. 3B).

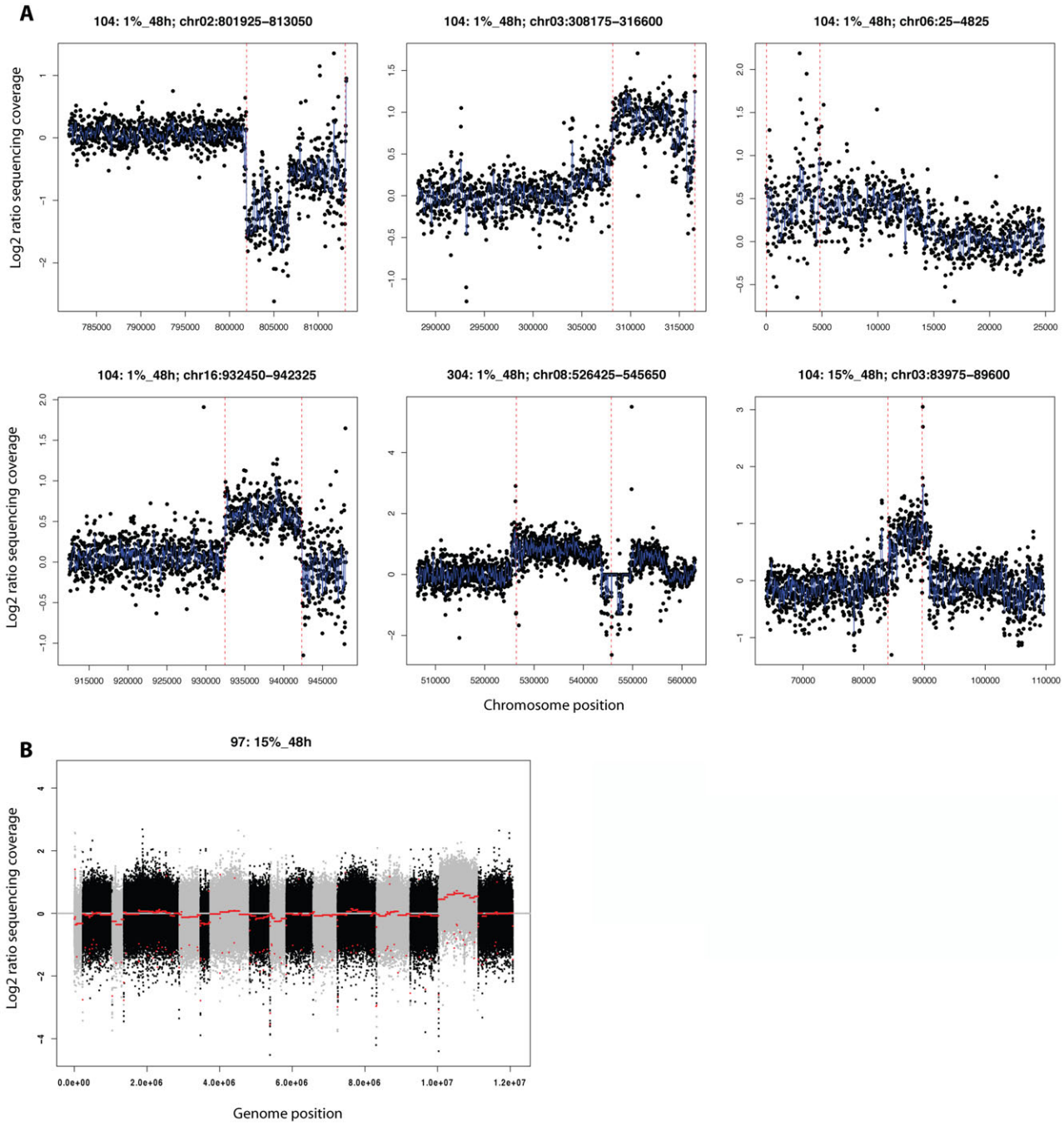

Figure 2. **Copy number variants (CNVs) identified by sequencing coverage of the evolved strain versus the ancestral strain. (A) Zoomed-in coverage plots of each subchromosomal CNV. Red dotted lines delimit the regions identified as CNVs by DNAcopy. Blue line is a running median of $\log_2$ ratios. CNVs occurred in three strains YPS128, YJM981, Y55, respectively, encoded 104, 304, and 97 on the figure. (B) Whole-genome coverage plot for the 97: 15%_48h evolved strain, showing duplication of chromosome 15. Alternating gray/black colors are chromosomes. Red line is a running median of $\log_2$ ratios.**

PHENOTYPIC EFFECT OF *BMH1* MUTATIONS

The distribution of the two classes of *BMH1* mutations (truncation vs. amino acid changes) was different between the two media although not statistically significant (Fisher's exact test, $P = 0.06$). Nonsense mutations, resulting in truncated proteins, were observed only in the 1% glucose medium (Table 6). From the predicted 3D protein structure, these truncated proteins will lack the final helix of the C-terminus as well as a glutamine repeat known to be involved in protein/protein interactions (Fig. 3C). Observed nonsynonymous mutations lead to amino acid changes at

Table 5. GO terms significantly enriched in the mutated gene set.

Selection regime	GO terms	GO ID	*P*-value	Expected FP	Gene(s) annotated to the term
All	Signal transduction	7165	0.00023	0	*MTH1*, *PKH1*, *BMH1*, *CYR1*, *CDC25*, *SSK2*, *SOG2*
	Intracellular signal transduction	35556	0.00296	0.04	*PKH1*, *BMH1*, *CYR1*, *CDC25*, *SSK2*
	Ras protein signal transduction	7265	0.02499	0.34	*BMH1*, *CYR1*, *CDC25*
1%_48h	Signal transduction	7165	0.0002	0	*PKH1*, *BMH1*, *CYR1*, *SSK2*, *SOG2*
	Intracellular signal transduction	35556	0.0007	0	*PKH1*, *BMH1*, *CYR1*, *SSK2*
	MAPKKK cascade	165	0.02237	0.1	*PKH1*, *SSH2*
	Cellular response to stimulus	51716	0.04528	0.16	*PKH1*, *BMH1*, *CYR1*, *SSK2*, *SOG2*
15%_48h (protein modifying mutations only)	Mitotic cell cycle	278	0.04208	0.24	*TPD3*, *BMH1*, *TVP38*, *CDC25*

Table 6. Distribution of the 13 Bmh1p mutations. There are two different ancestral sequences of Bmh1p (W1 and W2), one in S288C, Y55, YJM981 strains, the other in YPS128, NCYC110, UWOP83-787.3 strains.

	Selection regimes			
Ancestor strain	1%_48h	1%_96h	15%_48h	15%_96h
S288c				
Y55	E214stop Y216stop	2 x K217stop		D101N
YJM981	L230stop N178K	E214stop		
YPS128				
NCYC110				
UWOP83-787.3	G174V		G174D N178S G55D	

positions 55, 101, 174, 178 of the protein (Table 6) and were found in strains evolved in both glucose concentrations. Amino acid changes at 55, 174, and 178 are located inside the groove where Bmh1p is expected to interact with other proteins as predicted by docking with arbitrary peptides and with two known Bmh1p partners (the serine/threonine-protein phosphatase PP1-2 and the heat shock protein Ssb1).

We tested the effect of *BMH1* mutations on the value of each of the 13 traits separately. We distinguished five classes of Bmh1p: the ancestral sequences of strains S288c, Y55, YJM981, the ancestral sequences of strains of YPS128, NCYC110, UWOP83-787.3, the proteins truncated by stop mutations, the proteins having amino acid substitutions pointing toward the groove, and the protein having the unique amino acid substitution pointing toward the back inside. The last three classes of *BMH1* mutations changed the phenotypic value of a similar set of traits: R_{ferm}, T_{shift}, S_{ferm}, and R_{resp} (Fig. 4, Table 7). Interestingly, knowing the class of *BMH1* mutation provides as good or better prediction of the variation of these traits than knowing the ancestral strain (ANOVA's R^2 comparison, Table 7). Globally, the mutation effects were clearer in 15% evaluation medium than in 1%. In 15% glucose medium, substitutions G55D, G174D, and N178S, which are located in the Bmh1p groove of strain UWOP83-787.3, decreased average R_{ferm} ($P = 0.026$), increased T_{shift} ($P = 0.01$), and R_{resp} ($P = 0.047$), when compared to the ancestral protein sequence W2. Interestingly, the substitution D101N located in the back of the protein in strain Y55 also had an effect on T_{shift} and R_{ferm} (decreased R_{ferm}, $P = 0.05$, increased T_{shift}, $P = 0.019$). The effects of stop mutations were opposite to the effects of amino acid substitutions: they increased R_{ferm} ($P = 0.013$ for populations evolved in 1%_48h, $P = 0.168$ for populations evolved in 1%_96h), decreased T_{shift} ($P = 0.02$ for populations evolved in 1%_48h, $P = 0.056$ for populations evolved in 1%_96h), and increased S_{ferm} ($P = 0.086$ for populations evolved in 1%_48h, $P = 0.047$ for populations evolved in 1%_96h). Because stop mutations only occurred in the 1% selection regimes, we also analyzed whether the effect of stop mutations changed as a function of the evaluation medium. We found that stop mutations had antagonistic effects in 15% and 1% glucose media: while stop

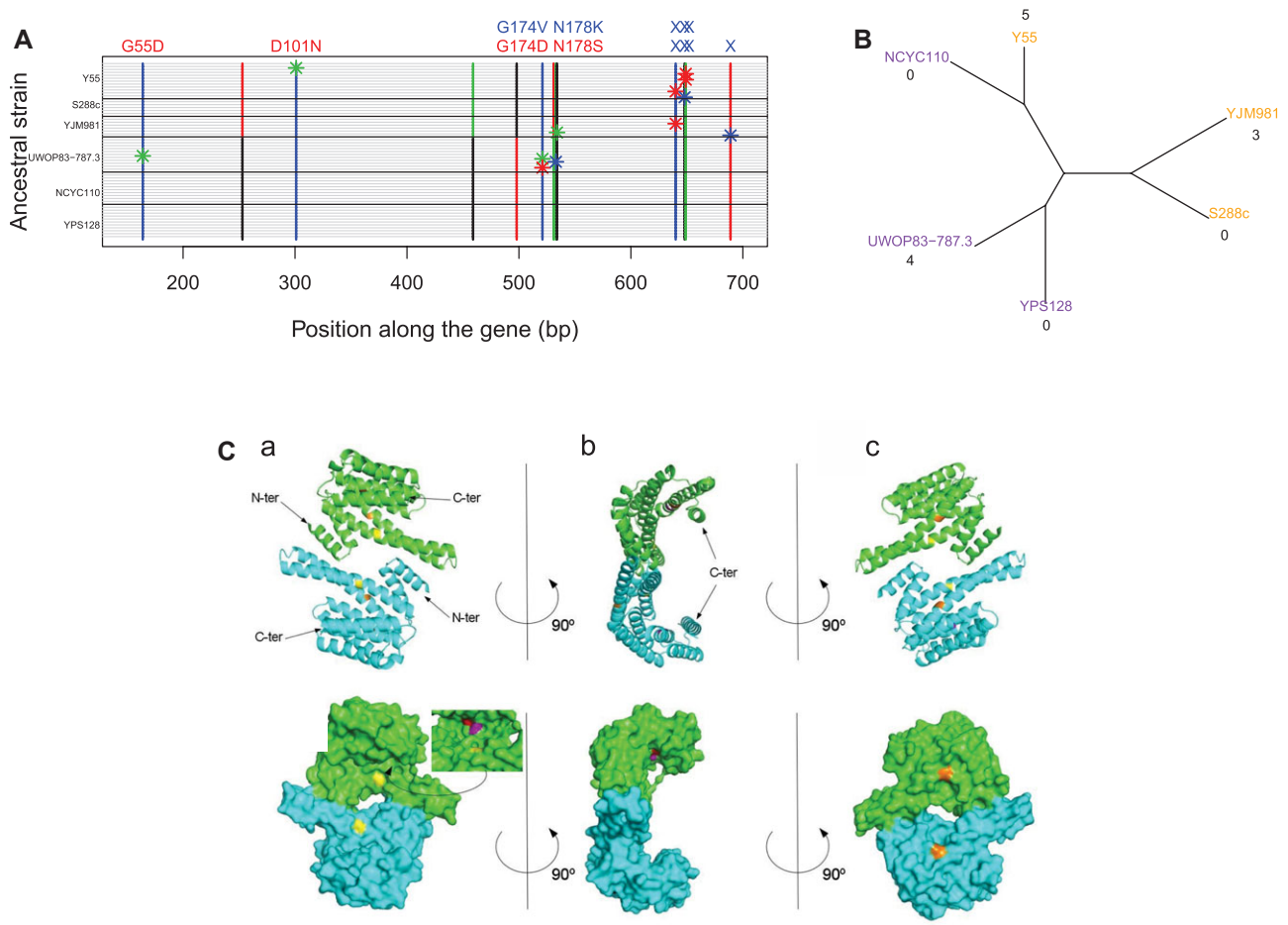

Figure 3. **Polymorphism in the *BMH1* gene and encoded protein. (A) Each gray horizontal line represents the allele sequence of a clone isolated from a population after evolution. The ancestral strain is shown on the left. Polymorphic sites are shown with vertical lines. Nucleotides are indicated with color (T in red, A in green, C in blue, G in black). Bars represent the ancestral allele and stars show mutations that had occurred along the evolutionary course. Corresponding changes in the protein are indicated on top of the nucleotide mutations. Crosses are stop mutations. Amino acid substitutions are indicated by their position in the protein. Mutations that have occurred in 1% selection regimes are indicated in blue, mutations that have occurred in 15% selection regimes in red. (B) Neighbor-joining tree based on the proportion of different nucleotides between genomes of the six ancestral strains. The *BMH1* allele is indicated by the color of the strain's name (orange or purple). The number of mutations that has occurred in *BMH1* during the course of evolution is indicated below the name of each strain. (C) Model of dimeric Bmh1p (region 1 to 235). A, front view; B, side view; C, back view; top row, cartoon representation; bottom row, surface representation. The two chains composing the dimer are shown in different colors (cyan and green). The positions affected by the mutation are highlighted in colors: position 55 in yellow, position 101 in orange, position 174 in red, and position 178 in purple.**

mutations increased R_{ferm} and decreased T_{shift} in 15% glucose media, they decreased R_{ferm} and increased T_{shift} in 1% glucose media. Note that stop mutations were selected in media where their effect on the reproduction rate was negative, demonstrating that reproduction rate is not always the best proxy for fitness.

Discussion

By varying both the environment and genetic background during experimental evolution, we found direct evidence of genotypic and phenotypic convergence in multiple traits by diverse genotypes selected in common environments, and of their divergence in differing environments.

DIVERGENT EVOLUTION BETWEEN ENVIRONMENTS

We found that each environment selected for a different combination of trait values, indicating that diversifying selection had occurred between the four selection regimes for various life-history and metabolic traits. In yeast, natural populations (from oak, soil) are characterized by large, fast-growing populations of small cells, whereas domesticated populations (from beer, wine,

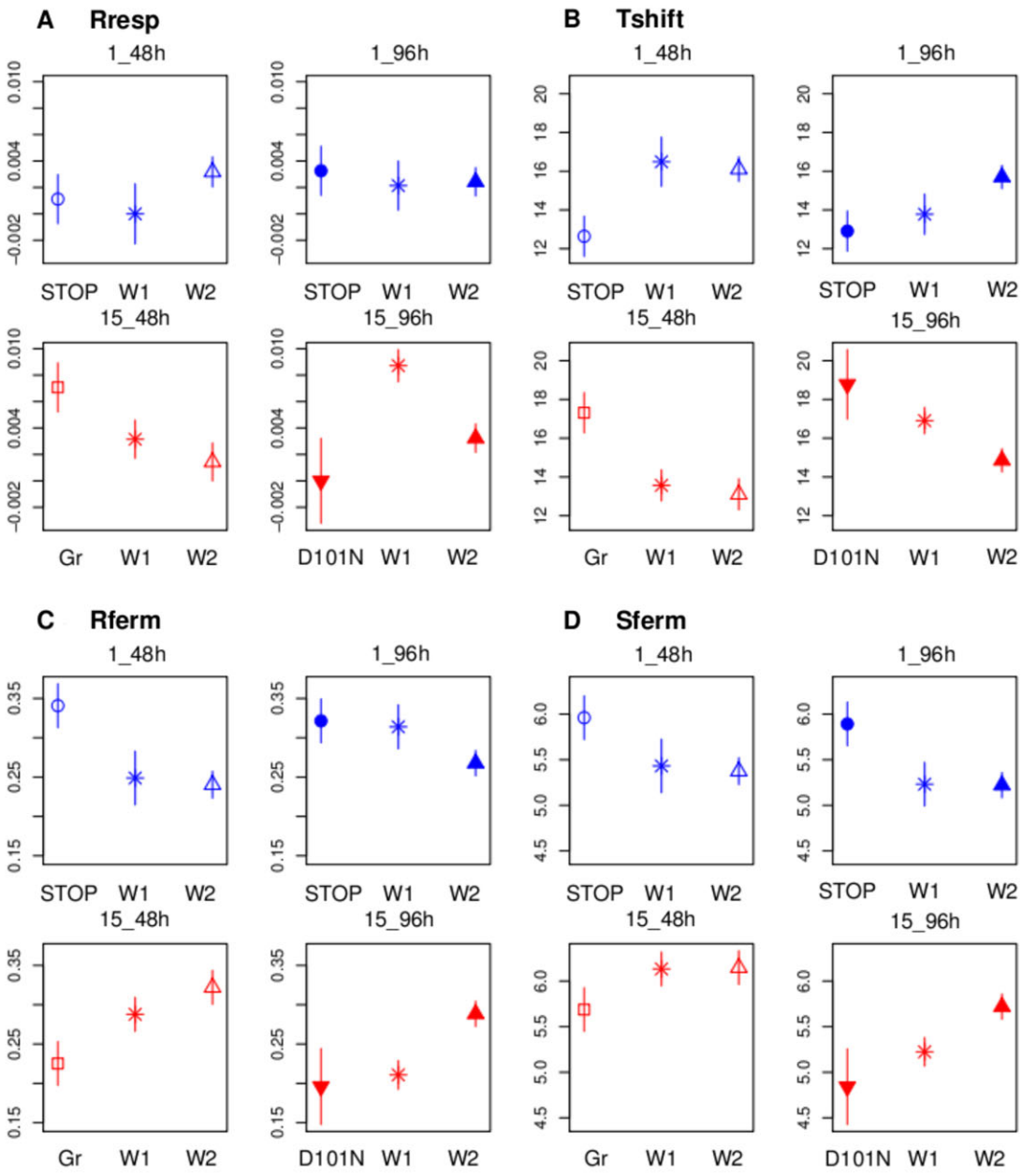

Figure 4. Effect of Bmh1p mutations in each selection regime where the mutations had occurred as evaluated in 15% glucose medium. W indicates evolved populations that have kept their ancestral protein sequences (W1 or W2), Gr indicates evolved populations that have had a substitution pointing on the groove of the protein, STOP indicates evolved populations having a truncated protein.

bread) are smaller, lower growing populations of big cells (Spor et al, 2008, 2009; Albertin et al. 2011). Here, by decreasing the amount of glucose and increasing the time of glucose starvation (1% _96h selection regime) in the laboratory, we selected for large, fast-growing populations of small cells in comparison to environments with high sugar availability. By analyzing evolution in action, we provide direct evidence that differences in sugar availability, as found between forest and domesticated environments, may explain the variation in life-history traits found in different yeast ecological niches.

CONVERGENT EVOLUTION IN PHENOTYPE AND GENOTYPE

Phenotypic convergent evolution is a well-documented phenomenon that shapes the adaptation of diverged organisms evolving in a common niche. Most studies investigating phenotypic convergence have focused on a single trait and/or a single environment. Here, we provide direct experimental support for multitrait convergence in response to selection in four different environments. We chose ancestral strains that were widely distributed on the *S. cerevisiae* phylogenomic tree (Liti et al. 2009)

Table 7. Testing the effect of Bmh1p mutations. Two ANOVA models were carried out, the first one with ancestor strains as genetic information, the other one with Bmh1p class of sequences as genetic information.

Traits	R^2 Strains model	R^2 Bmh1p model	*P*-value *Bbmh1p*	*P*-value *Bmh1p selection regime*	*P*-value *Bmh1p eval medium*	*P*-value *Bmh1p eval medium selection regime*
PopSize48h	0.607	0.295	0.979	0.967	0.853	0.769
PopSize96h	0.572	0.194	0.624	0.683	0.232	0.707
K_{ferm}	0.543	0.350	0.704	0.541	0.067	0.976
S_{ferm}	0.783	0.292	0.156	0.038	0.365	0.979
S48h	0.853	0.535	0.722	0.138	0.611	0.755
S96h	0.664	0.317	0.178	**0.015**	0.650	0.681
R_{ferm}	**0.324**	**0.266**	0.522	0.551	0.132	**0.034**
R_{resp}	**0.173**	**0.180**	0.054	0.476	**0.015**	0.863
T_{shift}	**0.486**	**0.464**	0.125	0.062	0.048	**0.022**
J_{spec}	0.789	0.712	0.194	0.886	0.741	0.778
Y_{ferm}:1%	0.349	0.130	NA	NA	0.053	0.428
Y_{ferm}:15%	0.587	0.222	NA	NA	0.632	**0.005**
Eth_48h:1%	0.448	0.393	NA	NA	0.403	0.328
Eth_48h:15%	0.107	0.069	NA	NA	0.709	0.120
Eth_96h:1%	−0.020	−0.188	NA	NA	0.912	0.912
Eth_96h:15%	**0.763**	**0.633**	NA	NA	**0.002**	0.939

The first column presents the R^2 of the first model. The other columns show the R^2 of the second model as well as the *P* value associated with the Bmh1p main and interactions effects. Significant effects after FDR correction are highlighted in bold.

that were also phenotypically divergent for their life-history and metabolic traits (Spor et al. 2009). Despite this diversity, strains evolved toward a common phenotype in each selection regime. In *Escherichia coli*, Fong et al. demonstrated parallel genotypic evolution and convergent growth phenotypes after evolving nine replicates of a single strain in two environmental conditions (Fong et al. 2005). Our study extends these findings to show that phenotypic convergence occurred between different genetic backgrounds.

After sequencing the genomes in a subset of our evolved strains, we find evidence that the same pathways, genes, and even nucleotides are recurrently mutated. By contrast, we did not find evidence of repeated CNVs events. The Ras/cAMP/PKA pathway and protein phosphatase 2A (PP2A) complex are repeated targets, with mutations in the genes *BMH1, CDC25, CYR1* and *TPD3, PPM1*, respectively. The gene *BMH1* is mutated in at least 20% of the populations, and four sites were mutated independently twice. These repeated mutational events strongly suggest that phenotypic convergence can be caused by convergence at the genotypic and pathway level. Mutations in the Ras/cAMP pathway had already been found in many other evolution experiments performed using glucose limitation in chemostats (Kao and Sherlock 2008; Kvitek and Sherlock 2011; Wenger et al. 2011), indicating that this pathway is a frequent target of adaptive mutation both in continuous and batch culture.

Finding recurrent mutations in *BMH1* was unexpected, and to our knowledge no previous experimental evolution studies have discovered adaptive mutations in this gene (e.g., Gresham et al. 2008; Lang et al. 2013). *BMH1* is highly pleiotropic, and has been shown to bind at least 271 proteins (Kakiuchi et al. 2007). Molecular analyses have implicated it in many functions, such as a chaperone-like protein, a protein tether, cell signaling, cell cycle control, transcriptional regulation, post-transcriptional regulation, life span, and apoptosis (Aitken 2006; van Heusden and Steensma 2006; Bruckmann et al. 2007; van Heusden 2009; Wang et al. 2009; Clapp et al. 2012; Veisova et al. 2012). Here, we showed that *BMH1* has an impact on the reproduction rate in fermentation and respiration, the length of fermentation (until the diauxic shift), and on cell size. Which of the traits controlled by Bmh1p have been selected for in our experiments remains to be studied.

We also see evidence for phenotypic convergence caused by mutations in disparate pathways in the 15%_48h condition. Mutations in genes within the PP2A complex (*TPD3, PPM1*), the Ras pathway/network (*CDC25, BMH1*), the glucose sensing pathway (*MTH1*), and membrane potential/cytoplasmic pH regulation (*HRK1*) are all likely causative mutations. However, each mutation affects a different pathway, with multiple pathways often being mutated in individual clones, suggesting that disparate genetic changes can converge on a common phenotype. Fong et al. (2005) demonstrated that the transcriptional states of their evolved

populations were very different from each other, despite similarity in endpoint growth phenotypes. They also showed that the evolutionary response involved an initial widespread expression shift followed by a large number of compensatory gene expression changes. Recently, other studies have also highlighted that phenotypic convergence could be achieved through diverse genetic mechanisms (Steiner et al. 2009; Chou and Marx 2012).

THE CAUSE OF CONVERGENCE

It is a common debate whether convergent evolution occurs because of natural selection toward a common adaptive phenotype, or for reasons unrelated to adaptation such as random evolutionary changes or constraints inherent to the biological system (DePristo et al. 2005; Weinreich 2006; Gompel and Prud'homme 2009; Feldman et al. 2012). Here, we provide strong evidence of convergent phenotypic and genotypic evolution occurring because of adaptation.

We show that mutations in a single gene converge specifically in one environment and have antagonistic effects in other environments, which is strong evidence that convergence occurred due to selection. Other mutations in the same gene, even at the same site, occurred and were selected for in different genetic backgrounds and in different environments. In addition, we show that positions of the mutations in *BMH1* appear to be nonrandom. None of the changes are located in the N-terminus of the protein, which is involved in dimerization. Instead, observed missense and nonsense mutations are predicted to be located in regions where protein–protein interactions occur and may change the capacity for interaction of Bmh1p with its potential partners. Finally, by simulating our experimental evolution under the neutral hypothesis, we show that such genetic convergence is unlikely without selection.

Genotypic convergence is thought to occur because of variation in adaptive potential between loci: variation in mutation rate, variation in the magnitude of mutation effect, variation in the number, and type of traits controlled directly or indirectly by the locus (pleiotropy, epistasy). Theoretical studies (Chevin et al. 2010) have shown that the probability of parallel evolution is increased when pleiotropy increased. Here we found that among eight genomes, the only gene that we observed to be mutated independently several times is highly pleiotropic.

THE EFFECT OF HISTORICAL CONTINGENCY

We showed that phenotypic and genotypic evolution depended on the ancestor. This was true for all but two life-history traits (R_{resp} and R_{ferm} in 15% evaluation medium), for all but two metabolic traits (T_{shift} in 1% evaluation medium and *Eth48h*, Table S1), as well as for the occurrence of selected mutations in *BMH1* (Table 6). The probability of occurrence of CNVs may also be contingent on the genetic background, because five of six CNVs were found in YPS128. The influence of the initial genotypes remains apparent even if adaptive convergence within a selection regime occurred; in fact, the phenotypic evolution was better explained by initial genotype than by selection regime for most traits (Table S1). Previous studies have suggested that historical contingency has more influence on traits with lesser fitness effects (Joshi et al. 2003; Travisano et al. 2005). Here, we present the most complete study thus far for testing this idea by including the analysis of many different cellular levels: genomic, metabolic, morphological, and reproduction traits. By contrast to previous studies, we found that the ancestors effect persists for most traits' and has not disappeared for traits that are strongly selected for. This probably reflects the fact that selection has not yet driven the populations to an adaptive peak and has not yet eliminated historical contingency. This can be partly explained by genetic convergence occurring in highly pleiotropic genes limiting the effect of selection on each trait separately, as illustrated by convergence on *BMH1*. All together, our data highlight the role of epistasis and pleiotropy into life-history evolution.

FITNESS LANDSCAPE IN MICROBES

The fitness landscape topology found here corresponds to a rugged landscape with various connected peaks organized around a convergent point. Whether fitness peaks are reached in our experiment remains to be studied, though seems unlikely given the relatively few generations elapsed in the experiments. Ruggedness has been related to a high level of epistasis (Kvitek and Sherlock 2011). We show here that it is also related to constraints emerging from pleiotropy. By and large, researchers have used the noncompetitive reproduction rate (also called growth rate) as a proxy for evolutionary fitness in microbes (Orr 2009). It remains debatable how accurate of a proxy this is, because selection can impact traits other than reproduction rate, such as the combination of traits representing fitness, often referred to as life-history traits (Roff 2002). For example, it has been shown that a simple increase in reproduction rate does not have to reflect the advantage of diploids over haploids in experimental evolution (Gerstein and Otto 2011). Similarly, in our case, the 15%_96h selection regime did not select for a higher reproduction rate during fermentation (R_{ferm}). Instead, it selected for a decreased population size, increased cell size and increase in specific glucose consumption rate, phenotypes that suggest the cells are not increasing reproduction rate but instead are metabolizing the abundant glucose to create biomass. Thus, phenotypic adaptation of multiple traits should be considered when investigating the fitness landscape of evolved microbial populations.

In conclusion, by analyzing evolution in action and its genotypic underpinnings, we found direct evidence of both convergent evolution in a particular environment and divergent selection among contrasted environments. In addition, we highlight

the need to analyze multiple fitness components for a better understanding of adaptation. We demonstrated examples of distinct genetic changes from disparate genetic backgrounds converging on a common phenotype, as well as these disparate genetic backgrounds finding convergent genotypic solutions. Finally we show that genotypic convergence underlying multiple traits' evolution is constrained by historical contingency and depends on the environment.

ACKNOWLEDGMENTS

The authors would like to thank G. Liti for kindly providing strains and the reviewers for critical reading of the manuscript. We are also grateful to M. Brockhurst, the GQF team, and F. Rosenzweig for fruitful discussions. Part of this work was supported by the CNRS.

DATA ARCHIVING

The doi for our data is 10.5061/dryad.j0k50.

LITERATURE CITED

Aitken, A. 2006. 14–3–3 proteins: a historic overview. Semin. Cancer Biol. 16:162–172.

Albertin, W., P. Marullo, M. Aigle, C. Dillmann, D. de Vienne, M. Bely, and D. Sicard. 2011. Population size drives industrial *Saccharomyces cerevisiae* alcoholic fermentation and is under genetic control. Appl. Environ. Microbiol. 77:2772–2784.

Araya, C., C. Payen, M. Dunham, and S. Fields. 2010. Whole-genome sequencing of a laboratory-evolved yeast strain. BMC Genomics 11:88.

Arendt, J., and D. Reznick. 2008. Convergence and parallelism reconsidered: what have we learned about the genetics of adaptation? Trends Ecol. Evol. 23:26–32.

Arnold, S. J., M. E. Pfrender, and A. G. Jones. 2001. The adaptive landscape as a conceptual bridge between micro- and macroevolution. Genetica 112:9–32.

Auesukaree, C., A. Damnernsawad, M. Kruatrachue, P. Pokethitiyook, C. Boonchird, Y. Kaneko, and S. Harashima. 2009. Genome-wide identification of genes involved in tolerance to various environmental stresses in *Saccharomyces cerevisiae*. J. Appl. Genet. 50:301–310.

Bedhomme, S., G. Lafforgue, and S. F. Elena. 2012. Multihost experimental evolution of a plant RNA virus reveals local adaptation and host-specific mutations. Mol. Biol. Evol. 29:1481–1492.

———. 2013. Genotypic but not phenotypic historical contingency revealed by viral experimental evolution. BMC Evol. Biol. 13:1–13.

Benjamini, Y., and Y. Hochberg. 1995. Controlling the false discovery rate—a practical and powerful approach. J. R. Stat. Soc. Ser. B 57: 289–300.

Bertram, P. G., C. Zeng, J. Thorson, A. S. Shaw, and X. F. Zheng. 1998. The 14–3–3 proteins positively regulate rapamycin-sensitive signaling. Curr. Biol. 8:1259–1267.

Blount, Z. D., C. Z. Borland, and R. E. Lenski. 2008. Historical contingency and the evolution of a key innovation in an experimental population of *Escherichia coli*. Proc. Natl. Acad. Sci. USA 105:7899–7906.

Boyle, E. I., S. Weng, J. Gollub, H. Jin, D. Botstein, J. M. Cherry, and G. Sherlock. 2004. GO::TermFinder—open source software for accessing Gene Ontology information and finding significantly enriched Gene Ontology terms associated with a list of genes. Bioinformatics 20:3710–3715.

Broek, D., T. Toda, T. Michaeli, L. Levin, C. Birchmeier, M. Zoller, S. Powers, and M. Wigler. 1987. The *S. cerevisiae CDC25* gene product regulates the *RAS*/adenylate cyclase pathway. Cell 48:789–799.

Bruckmann, A., P. J. Hensbergen, C. I. A. Balog, A. M. Deelder, H. Y. Steensma, and G. P. H. van Heusden. 2007. Post-transcriptional control of the *Saccharomyces cerevisiae* proteome by 14–3–3 proteins. J. Proteome Res. 6:1689–1699.

Bull, J. J., M. R. Badgett, H. A. Wichman, J. P. Huelsenbeck, D. M. Hillis, A. Gulati, C. Ho, and I. J. Molineux. 1997. Exceptional convergent evolution in a virus. Genetics 147:1497–1507.

Burbelo, P. D., and A. Hall. 1995. 14–3–3 proteins: hot numbers in signal transduction. Curr. Biol. 5:95–96.

Chevin, L.-M., G. Martin, and T. Lenormand. 2010. Fisher's model and the genomics of adaptation: restricted pleiotropy, heterogenous mutation, and parallel evolution. Evolution 64:3213–3231.

Chou, H.-H., and C. J. Marx. 2012. Optimization of gene expression through divergent mutational paths. Cell Rep. 1:133–140.

Christin, P.-A., N. Salamin, V. Savolainen, M. R. Duvall, and G. Besnard. 2007. C4 photosynthesis evolved in grasses via parallel adaptive genetic changes. Curr. Biol. 17:1241–1247.

Clapp, C., L. Portt, C. Khoury, S. Sheibani, G. Norman, P. Ebner, R. Eid, H. Vali, C. A. Mandato, F. Madeo et al. 2012. 14–3–3 protects against stress-induced apoptosis. Cell Death Dis. 3:e348.

Cunningham, C. W., K. Jeng, J. Husti, M. Badgett, I. J. Molineux, D. M. Hillis, and J. J. Bull. 1997. Parallel molecular evolution of deletions and nonsense mutations in bacteriophage T7. Mol. Biol. Evol. 14:113–116.

David, L., Y. Ben-Harosh, E. Stolovicki, L. S. Moore, M. Nguyen, R. Tamse, J. Dean, E. Mancera, L. M. Steinmetz, and E. Braun. 2013. Multiple genomic changes associated with reorganization of gene regulation and adaptation in yeast. Mol. Biol. Evol. 30:1514–1526.

DePristo, M. A., D. M. Weinreich, and D. L. Hartl. 2005. Missense meanderings in sequence space: a biophysical view of protein evolution. Nat. Rev. Genet. 6:678–687.

Dunn, B., C. Richter, D. J. Kvitek, T. Pugh, and G. Sherlock. 2012. Analysis of the *Saccharomyces cerevisiae* pan-genome reveals a pool of copy number variants distributed in diverse yeast strains from differing industrial environments. Genome Res. 22:908–924.

Elias, M., and D. S. Tawfik. 2012. Divergence and convergence in enzyme evolution: parallel evolution of paraoxonases from quorum-quenching lactonases. J. Biol. Chem. 287:11–20.

Elmer, K. R., and A. Meyer. 2011. Adaptation in the age of ecological genomics: insights from parallelism and convergence. Trends Ecol. Evol. 26:298–306.

Feldman, C. R., E. D. Brodie, E. D. Brodie, and M. E. Pfrender. 2012. From the cover: constraint shapes convergence in tetrodotoxin-resistant sodium channels of snakes. Proc. Natl. Acad. Sci. USA 109:4556–4561.

Fong, S. S., A. R. Joyce, and B. Ø. Palsson. 2005. Parallel adaptive evolution cultures of *Escherichia coli* lead to convergent growth phenotypes with different gene expression states. Genome Res. 15:1365–1372.

Gerstein, A. C., and S. P. Otto. 2011. Cryptic fitness advantage: diploids invade haploid populations despite lacking any apparent advantage as measured by standard fitness assays. PLoS One 6:e26599.

Gompel, N., and B. Prud'homme. 2009. The causes of repeated genetic evolution. Dev. Biol. 332:36–47.

Granek, J. A., Ö. Kayıkçı, and P. M. Magwene. 2011. Pleiotropic signaling pathways orchestrate yeast development. Curr. Opin. Microbiol. 14:676–681.

Gresham, D., M. M. Desai, C. M. Tucker, H. T. Jenq, D. A. Pai, A. Ward, C. G. DeSevo, D. Botstein, and M. J. Dunham. 2008. The repertoire and dynamics of evolutionary adaptations to controlled nutrient-limited environments in yeast. PLoS Genet. 4:e1000303.

Herron, M. D., and M. Doebeli. 2013. Parallel evolutionary dynamics of adaptive diversification in *Escherichia coli*. PLoS Biol. 11:e1001490.

Hoebeeck, J., F. Speleman, and J. Vandesompele. 2007. Real-time quantitative PCR as an alternative to Southern blot or fluorescence in situ hybridization for detection of gene copy number changes. Methods Mol. Biol. 353:205–226.

Jorgensen, P. 2002. Systematic identification of pathways that couple cell growth and division in yeast. Science 297:395–400.

Joshi, A., R. B. Castillo, and L. D. Mueller. 2003. The contribution of ancestry, chance, and past and ongoing selection to adaptive evolution. J. Genet. 82:147–162.

Kakiuchi, K., Y. Yamauchi, M. Taoka, M. Iwago, T. Fujita, T. Ito, S.-Y. Song, A. Sakai, T. Isobe, and T. Ichimura. 2007. Proteomic analysis of in vivo 14–3–3 interactions in the yeast *Saccharomyces cerevisiae*†. Biochemistry 46:7781–7792.

Kao, K. C., and G. Sherlock. 2008. Molecular characterization of clonal interference during adaptive evolution in asexual populations of *Saccharomyces cerevisiae*. Nat. Genet. 40:1499–1504.

Kolbe, J. J., L. J. Revell, B. Szekely, E. D. Brodie III, and J. B. Losos. 2011. Convergent evolution of phenotypic integration and its alignment with morphological diversification in Caribbean anolis ectomorphs. Evolution 65:3608–3624.

Kumar, P., S. Henikoff, and P. C. Ng. 2009. Predicting the effects of coding non-synonymous variants on protein function using the SIFT algorithm. Nat. Protoc. 4:1073–1081.

Kvitek, D. J., and G. Sherlock. 2011. Reciprocal sign epistasis between frequently experimentally evolved adaptive mutations causes a rugged fitness landscape. PLoS Genet. 7:e1002056.

Lang, G. I., D. P. Rice, M. J. Hickman, E. Sodergren, G. M. Weinstock, D. Botstein, and M. M. Desai. 2013. Pervasive genetic hitchhiking and clonal interference in forty evolving yeast populations. Nature 500:571–574.

Li, H., and R. Durbin. 2009. Fast and accurate long-read alignment with Burrows-Wheeler transform. Bioinformatics 26:589–595.

Li, H., B. Handsaker, A. Wysoker, T. Fennell, J. Ruan, N. Homer, G. Marth, G. Abecasis, R. Durbin, and 1000 Genome Project Data Processing Subgroup. 2009. The Sequence Alignment/Map format and SAMtools. Bioinformatics 25:2078–2079.

Liti, G., D. M. Carter, A. M. Moses, J. Warringer, L. Parts, S. A. James, R. P. Davey, I. N. Roberts, A. Burt, V. Koufopanou et al. 2009. Population genomics of domestic and wild yeasts. Nature 458:337–341.

Lozovsky, E. R., T. Chookajorn, K. M. Brown, M. Imwong, P. J. Shaw, S. Kamchonwongpaisan, D. E. Neafsey, D. M. Weinreich, and D. L. Hartl. 2009. Stepwise acquisition of pyrimethamine resistance in the malaria parasite. Proc. Natl. Acad. Sci. USA 106:12025–12030.

Magwene, P. M., O. Kayikci, J. A. Granek, J. M. Reininga, Z. Scholl, and D. Murray. 2011. Outcrossing, mitotic recombination, and life-history trade-offs shape genome evolution in *Saccharomyces cerevisiae*. Proc. Natl. Acad. Sci. USA 108:1987–1992.

Manceau, M., V. S. Domingues, C. R. Linnen, E. B. Rosenblum, and H. E. Hoekstra. 2010. Convergence in pigmentation at multiple levels: mutations, genes and function. Philos. Trans. R. Soc. Lond. B 365: 2439–2450.

Martinez-Picado, J., M. P. DePasquale, N. Kartsonis, G. J. Hanna, J. Wong, D. Finzi, E. Rosenberg, H. F. Gunthard, L. Sutton, A. Savara et al. 2000. Antiretroviral resistance during successful therapy of HIV type 1 infection. Proc. Natl. Acad. Sci. USA 97:10948–10953.

McKenna, A., M. Hanna, E. Banks, A. Sivachenko, K. Cibulskis, A. Kernytsky, K. Garimella, D. Altshuler, S. Gabriel, M. Daly et al. 2010. The Genome Analysis Toolkit: a MapReduce framework for analyzing next-generation DNA sequencing data. Genome Res. 20:1297–1303.

Nguyen, A. H., I. J. Molineux, R. Springman, and J. J. Bull. 2012. Multiple genetic pathways to similar fitness limits during viral adaptation to a new host. Evolution 66:363–374.

Orr, H. A. 2009. Fitness and its role in evolutionary genetics. Nat. Rev. Genet. 10:531–539.

Ostrowski, E. A., R. J. Woods, and R. E. Lenski. 2008. The genetic basis of parallel and divergent phenotypic responses in evolving populations of *Escherichia coli*. Proc. R. Soc. Lond. B 275:277–284.

Parker, J., G. Tsagkogeorga, J. A. Cotton, Y. Liu, P. Provero, E. Stupka, and S. J. Rossiter. 2013. Genome-wide signatures of convergent evolution in echolocating mammals. Nature. 502:228–231.

Plata, E. R., and H. T. Lumbsch. 2011. Parallel evolution and phenotypic divergence in lichenized fungi: a case study in the lichen-forming fungal family Graphidaceae (Ascomycota: Lecanoromycetes: Ostropales). Mol. Phylogenet. Evol. 61:45–63.

Remold, S. K., A. Rambaut, and P. E. Turner. 2008. Evolutionary genomics of host adaptation in vesicular stomatitis virus. Mol. Biol. Evol. 25:1138–1147.

Roff, D. A. 2002. Life history evolution. Sinauer Associates, MA.

———. 2011. Genomic insights into life history evolution. Pp. 11–25 *in* Thomas Flatt and Andreas Heyland, eds. Mechanisms of life history evolution the genetics and physiology of life history traits and trade-offs. University of Oxford Press, Oxford, U.K.

Rosenblum, E. B., H. Rompler, T. Schoneberg, and H. E. Hoekstra. 2010. From the cover: molecular and functional basis of phenotypic convergence in white lizards at White Sands. Proc. Natl. Acad. Sci. USA 107:2113–2117.

Rozpędowska, E., L. Hellborg, O. P. Ishchuk, F. Orhan, S. Galafassi, A. Merico, M. Woolfit, C. Compagno, and J. Piškur. 2011. Parallel evolution of the make-accumulate-consume strategy in Saccharomyces and Dekkera yeasts. Nat. Commun. 2:302.

Schluter, D. 1996. Adaptive radiation along genetic lines of least resistance. Evolution 50:1766–1774.

Spor, A., S. Wang, C. Dillmann, D. de Vienne, and D. Sicard. 2008. "Ant" and "Grasshopper" life-history strategies in *Saccharomyces cerevisiae*. PLoS One 3:e1579.

Spor, A., T. Nidelet, J. Simon, A. Bourgais, D.deVienne, and D. Sicard. 2009. Niche-driven evolution of metabolic and life-history strategies in natural and domesticated populations of *Saccharomyces cerevisiae*. BMC Evol. Biol. 9:296.

Srithayakumar, V., S. Castillo, J. Mainguy, and C. J. Kyle. 2011. Evidence for evolutionary convergence at MHC in two broadly distributed mesocarnivores. Immunogenetics 64:289–301.

Steiner, C. C., H. Rompler, L. M. Boettger, T. Schoneberg, and H. E. Hoekstra. 2009. The genetic basis of phenotypic convergence in beach mice: similar pigment patterns but different genes. Mol. Biol. Evol. 26:35–45.

Tenaillon, O., A. Rodriguez-Verdugo, R. L. Gaut, P. McDonald, A. F. Bennett, A. D. Long, and B. S. Gaut. 2012. The molecular diversity of adaptive convergence. Science 335:457–461.

Teotónio, H., I. M. Chelo, M. Bradić, M. R. Rose, and A. D. Long. 2009. Experimental evolution reveals natural selection on standing genetic variation. Nat. Genet. 41:251–257.

Travisano, M., J. A. Mongold, A. F. Bennett, and R. E. Lenski. 2005. Experimental tests of the roles of adaptation, chance, and history in evolution. Science 267:87–90.

Treco. 1987. Current protocols in molecular biology. *In* F. M. Ausubel, R. Brent, R. E. Kingston, D.D. Moore, J. G. Seidman, J. A. Smith, and K. Struhl, eds. John Wiley, NY.

True, J. R., and E. S. Haag. 2001. Developmental system drift and flexibility in evolutionary trajectories. Evol. Dev. 3:109–119.

Van Heusden, G. P. H. 2009. 14–3–3 proteins: insights from genome-wide studies in yeast. Genomics 94:287–293.

Van Heusden, G. P. H., and H. Yde Steensma. 2006. Yeast 14–3–3 proteins. Yeast 23:159–171.

Van Zyl, W., W. Huang, A. A. Sneddon, M. Stark, S. Camier, M. Werner, C. Marck, A. Sentenac, and J. R. Broach. 1992. Inactivation of the protein phosphatase 2A regulatory subunit A results in morphological and transcriptional defects in *Saccharomyces cerevisiae*. Mol. Cell. Biol. 12:4946–4959.

Veisova, D., E. Macakova, L. Rezabkova, M. Sulc, P. Vacha, H. Sychrova, T. Obsil, and V. Obsilova. 2012. Role of individual phosphorylation sites for the 14–3–3-protein-dependent activation of yeast neutral trehalase Nth1. Biochem. J. 443:663–670.

Venkatraman, E. S., and A. B. Olshen. 2007. A faster circular binary segmentation algorithm for the analysis of array CGH data. Bioinformatics 23:657–663.

Wang, C., C. Skinner, E. Easlon, and S.-J. Lin. 2009. Deleting the 14–3–3 protein *BMH1* extends life span in *Saccharomyces cerevisiae* by increasing stress response. Genetics 183:1373–1384.

Wang, S., A. Spor, T. Nidelet, P. Montalent, C. Dillmann, D. de Vienne, and D. Sicard. 2011. Switch between life history strategies due to changes in glycolytic enzyme gene dosage in *Saccharomyces cerevisiae*. Appl. Environ. Microbiol. 77:452–459.

Weinreich, D. M. 2006. Darwinian evolution can follow only very few mutational paths to fitter proteins. Science 312:111–114.

Wenger, J. W., J. Piotrowski, S. Nagarajan, K. Chiotti, G. Sherlock, and F. Rosenzweig. 2011. Hunger artists: yeast adapted to carbon limitation show trade-offs under carbon sufficiency. PLoS Genet. 7:e1002202.

Wichman, H. A. 1999. Different trajectories of parallel evolution during viral adaptation. Science 285:422–424.

Wichman, H. A., J. Wichman, and J. J. Bull. 2005. Adaptive molecular evolution for 13,000 phage generations: a possible arms race. Genetics 170:19–31.

Wong, A., N. Rodrigue, and R. Kassen. 2012. Genomics of adaptation during experimental evolution of the opportunistic pathogen *Pseudomonas aeruginosa*. PLoS Genet 8:e1002928.

Wood, T. E., J. M. Burke, and L. H. Rieseberg. 2005. Parallel genotypic adaptation: when evolution repeats itself. Genetica 123:157–170.

Yang, X., W. H. Lee, F. Sobott, E. Papagrigoriou, C. Robinson, G. J. Grossmann, M. Sundström, D. Doyle, and J. Elkin. 2006. Structural basis for protein-protein interactions in the 14–3–3 protein family. Proc. Natl. Acad. Sci. USA 103:17237–17242.

Zhang, J., and S. Kumar. 1997. Detection of convergent and parallel evolution at the amino acid sequence level. Mol. Biol. Evol. 14:527–536.

Associate Editor: A. De Visser

Supporting Information

Additional Supporting Information may be found in the online version of this article at the publisher's website:

Table S1. Analyses of variance for each single trait.